STRUCTURAL INTEGRITY ASSESSMENTS OF AUSTENITIC STAINLESS STEEL PIPES WITH AXIAL FLAWS

Roberto Ferraboli Jr.
Graduate Student, Department of Naval Architecture and Ocean Engineering,
University of São Paulo, São Paulo, SP 05508–900, Brazil

Claudio Ruggieri
Professor, Department of Naval Architecture and Ocean Engineering,
University of São Paulo, São Paulo, SP 05508–900, Brazil
E–mail: claudio.ruggieri@poli.usp.br

Abstract – Current structural integrity assessment procedures based on failure analysys diagrams (FAD), such as BS7910 and API579 procedures, are now well established to evaluate the severity of crack-like defects in structural components made of ferritic steels. However, the application (and validation) of these procedures in defect assessments of structural components made of austenitic stainless steels still remains an open issue. The high strain hardening capacity and high ductility of austenitic stainless steels most often make these procedures unsuitable for integrity assessments of these materials. This work extends the applicability of failure analysis diagrams for failure assessments of austenitic steel pipes with axial flaws to include the effects of strain hardening properties and ductility. Full-scale burst tests are conducted on a 4 inch pipe made of AISI 304 steel containing different axial cracks to measure the failure pressure. The direct application of the API 579 and BS 7910 procedures indicate large margins between the predicted and the actual (measured) failure pressures. While such conservatism represents an extra factor of safety, excessive pessimism in defect assessments can lead to unwarranted repairs or replacement of in-service pipelines at great operational costs. These results provide support to develop more refined FAD procedures which are more applicable to austenitic stainless steels.

Keywords*: structural integrity, defect assessment, austenitic steels, burst pressure, FAD methodology*

1. Introduction

Austenitic stainless steel alloys are used extensively in heat-resistant structural components in power generating and chemical industries due to metallurgical stability, excellent corrosion resistance as well as good creep and ductility properties. Current design codes and standards for pressurized equipments provide rules for design, fabrication, inspection and testing of critical structures made of this class of alloys, including pressure vessels and piping systems. While these codes provide simplified acceptance criteria for fabrication defects (such as slag inclusions and porosity in weldments) based upon workmanship standards and full-scale hydrostatic testing, they not specifically address fitness-for-service (FFS) assesments of crack-like defects that form during in-service operation. Fracture mechanics based approaches, also referred to as Engineering Critical Assessment (ECA) procedures, remain essential in repair decisions and life-extension programs of in-service structural components.

Current structural integrity assessment procedures based on failure analysys diagrams (FAD), such as BS7910 [1] and API579 [2] procedures, are now well established to evaluate the severity of crack-like defects in structural components made of ferritic steels. However, the application (and validation) of these procedures in defect assessments of structural components made of austenitic stainless steels still remains an open issue. The high strain hardening capacity and high ductility of austenitic stainless steels most often make these procedures unsuitable for integrity assessments of these materials.

This work extends the applicability of failure analysis diagrams for failure assessments of austenitic steel pipes with axial flaws to include the effects of strain hardening properties and ductility. Full–scale burst tests are conducted on a 4 inch pipe made of AISI 304 steel containing different axial cracks to measure the failure pressure. The direct application of the API 579 and BS 7910 procedures indicate large margins between the predicted and the actual (measured) failure pressures. While such conservatism represents an extra factor of safety, excessive pessimism in defect assessments can lead to unwarranted repairs or replacement of in-service pipelines at great operational costs. These results provide support to develop more refined FAD procedures which are more applicable to austenitic stainless steels.

2. Overview of the FAD Methodology

It is widely recognized that brittle fracture and plastic collapse caused by overloading are competing failure modes in structural components made of materials with sufficient toughness. Early work by Dowling and Townley [3] and Harrison [4] to address the potential interaction between fracture and plastic collapse introduced the concept of a two-criteria failure assessment diagram (most often referred to as FAD) to describe the mechanical integrity of a cracked component. In the FAD methodology, a roughly geometry-independent failure line is constructed based upon a relationship between the normalized crack-tip loading and the material's fracture resistance (which include both modes of brittle fracture and overload fracture) in the form

$$K_r = f(L_r) \tag{1}$$

where

$$K_r = \frac{K_{\mathrm{I}}(P,a)}{K_{\mathrm{Ic}}} \tag{2}$$

$$L_r = \frac{P}{P_L(a,\sigma_{ys})} \tag{3}$$

Here P is the load applied to the component containing a defect of size a, K_{I} is the elastic stress intensity factor, K_{Ic} is the (plane-strain) fracture toughness, σ_{ys} is the yield stress and P_L is the value of P corresponding to plastic collapse of the component (which also depends on crack size).

Fittness-for-service (FFS) assessments of crack-like defects based upon the FAD philosophy have undergone extensive developments in the past decade. The most widely used FAD procedures which form the basis for industrial codes and guidelines for defect assessments are the R6 routine [5], BS 7910 [1] and API 579 [2]. In particular, the American Petroleum Institute (API) Recommended Practice 579 [2] has recently been developed to provide an FFS assessment procedure for flaws commonly found in pressure vessels, piping and storage tanks of the refining and petrochemical industry. It incorporates a three-tiered (or three-level) FAD criterion with increasing analytical sophistication and data requirements and decreasing conservatism. The main crack-like flaw assessment in API 569 and BS7910 is Level 2 which uses the following FAD expression

$$K_r = \left[1 - 0.14(L_r)^2\right]\left\{0.3 + 0.7\exp\left[-0.65(L_r)^6\right]\right\} \tag{4}$$

where the load ratio is now defined as

$$L_r = \frac{\sigma_{ref}}{\sigma_{ys}} \tag{5}$$

with σ_{ref} being defined as a reference stress which derives from a limit load solution.

Figure 1 illustrates the FAD concept for the Level 2 option given by API 579 [2]. The toughness ratio, K_r, and the load ratio, L_r, for the structural component under analysis are plotted on the diagram. The structural integrity assessment of the component is the based on the relative location of the assessment point with respect to the FAD curve. The component is simply considered safe if the assessment point lies below the FAD curve whereas it is considered *potentially* unsafe if the assessment point lies on or above the FAD curve. An increased laod or larger crack will move the assessment point along the loading path towards the failure line. The cut-off load parameter, L_r^{max}, is defined in terms of the material flow stress, $\tilde{\sigma}$, and yield stress as

$$L_r^{max} = \frac{\tilde{\sigma}}{\sigma_{ys}} \tag{6}$$

where the flow stress, $\tilde{\sigma}$, is often defined as the mean value of the yield stress, σ_{ys}, and the ultimate stress, σ_{uts}, thereby taking account of the hardening effect above yielding observed in ferritic carbon steels and austenitic stainless steels.

3. Material Description

To investigate the burst behavior in cracked pipes, full scale hydrostatic tests were performed on a 168 mm O.D tubular specimen with 7.11 mm wall thickness (ANSI 6 inch diameter Sch 40S). The material employed in this study is an austenitic stainless AISI 304 steel following specification ASTM A312 Grade TP 304. Table 1 shows the chemical composition for the tested steel. Mechanical tensile tests conducted on rectangular tensile specimens extracted from the pipe specimens (longitudinal direction) provide the mechanical

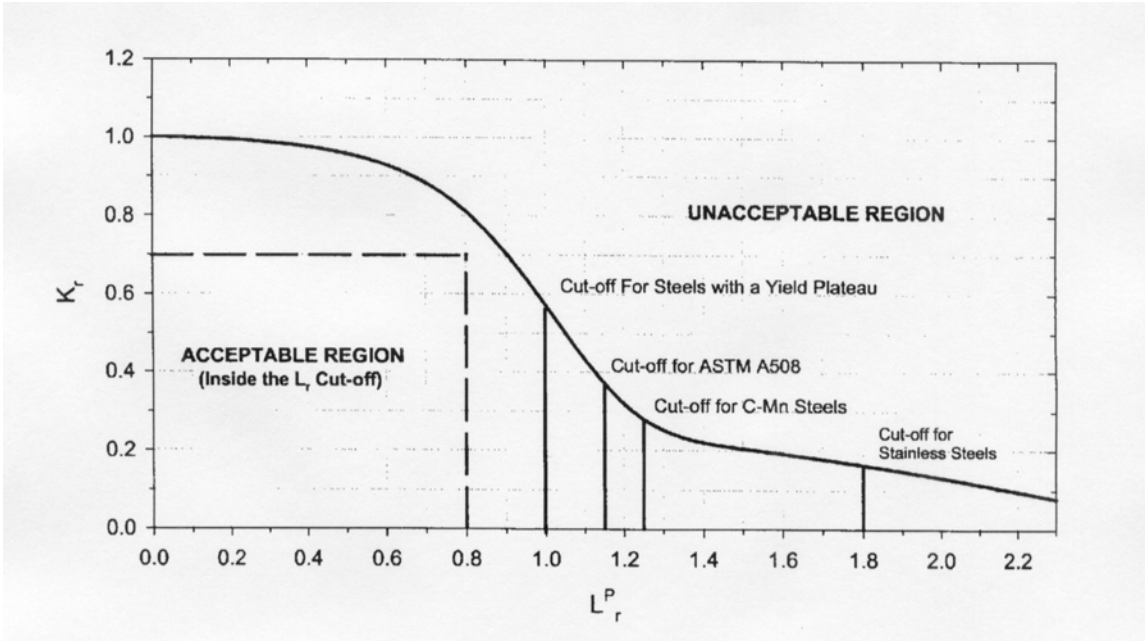

Figure 1 *Level 2 FAD for API 579 [2]*

properties at room temperature (20°C). Table 2 displays the measured tensile properties for the tested material

Table 1 Chemical composition of tested AISI 304 austenitic stainless steel (wt.%)

C	Si	Mn	P	S	Cr	Ni	Mo	V	Co
0.027	0.47	1.36	0.023	0.011	18.45	9,15	0.11	0.10	0.10

Table 2 Mechanical properties of tested AISI 304 austenitic stainless steel at room temperature

σ_{ys} (MPa)	σ_{uts} (MPa)	Elongation (%)	Elongation (%)
398	652	46	67

4. Experimental Measurements of Burst Pressure

To investigate the failure behavior of axially flawed pipes, a series of full scale burst tests were performed on end-capped pipe specimens with external diameter, $D_e = 168$ mm, wall thickness, $t = 7.11$ mm and length, $L = 6$ m. These experimental tests were conducted on pipe specimens with external longitudinal surface cracks with different sizes measured by crack depth and crack length, $a \times 2c$, and with a fixed crack depth of 2.55 mm ($a/t = 0.4$). The longitudinal flaws have dimensions 2.55×85 mm (A1), 2.55×127 mm (A2), 2.55×255 mm (A3), 2.55×21.25 mm (A4) and 2.55×10.65 mm (A5) where A1, A2, A3, A4 and A5 denotes the crack geometry. Figure 2(a) provides a schematic illustration of the pipe specimen with an external longitudinal flaw. Figure 2(b) shows a schematic illustration of the test rig employed for the hydrostatic testing. The pipe specimens were notched along their length using an electrical discharge machine (EDM) to create the required notch shape. The initial semi-elliptical defects were not subjected to a pressure cycle to propagate a fatigue crack from the original notch. However, the high accurate machining process allows

considering them as initially blunted cracks. Table 3 provides the experimentally measured burst pressures obtained from the hydrostatic tests. Figure 3 pictures a general view of pipe specimens A2 and A3 (with a longitudinal flaw of 2.55×127 mm and 2.55×255 mm) which shows the crack region and accompanying deformation (bulging) after pipe collapse.

Table 3 Experimentally measured burst pressure for tested pipes

Specimen / Crack Geometry	A1	A2	A3	A4	A5
Burst Pressure, P_B (MPa)	33.5	33.0	34.1	37.1	42.8

5. Burst Pressure Predictions Using the FAD Methodology

5.1. API 579

The FAD methodology based upon the API 579 procedure using Level 2 described in the previous section has been applied to predict the burst pressure for the tested pipe specimens. Following Section 9 of API 579 and Appendix D, the reference stress, σ_{ref}, for a pipe with a longitudinal crack is given by

$$\sigma_{ref} = M_S P_M \tag{7}$$

where P_M is the membrane stress acting on the crack face (opening mode) and parameter M_S is expressed by

$$M_S = \frac{1 - C(a/t)(1/M_t)}{1 - C(a/t)} \tag{8}$$

with factor C assigned a value of 0.85 and parameter M_t defined by

$$M_t = \left(\frac{1.02 + 0.4411\lambda^2 + 0.006124\lambda^4}{1.00 + 0.02642\lambda^2 + 1.533 \cdot 10^{-6}\lambda^4} \right)^{0.5} \tag{9}$$

where λ is

$$\lambda = \frac{1.818c}{\sqrt{R_i t}} \tag{10}$$

Here c is half-crack size, t is the pipe wall thickness and R_i is the internal radius (see Fig. 2(a)).

To determine the toughness ratio, K_r, the stress intensity factors for the axially cracke pipes is calculated from Appendix C of API 579 which contains an extensive library of stress intensity solutions for cracks in cylindrical and spherical shells. For the pipe specimen employed in this study, the stress intensity factor is given by

$$K_{\mathrm{I}} = \frac{pR_i^2}{R_o^2 - R_i^2} \left[2G_0 + 2G_1 \left(\frac{a}{R_i} \right) \right] \sqrt{\frac{\pi a}{Q}} \tag{11}$$

where p is the internal pressure, a is the crack depth, R_o is the outer radius and G_0 and G_1 are influence coefficients. The flaw shape parameter is defined as

$$Q = 1.0 + 1.464 \left(\frac{a}{c} \right)^{1.65} \tag{12}$$

The material toughness, K_{Ic}, is taken as 155 MPa$\sqrt{m}$ from reference [6] which is a rather conservative toughness value for this class of material. Ideally, a fracture mechanics test should be conducted to measure the (plane-strain) fracture toughness. However, the very stringent size limits imposed by ASTM E399 to get valid K_{Ic}-values make it impossible to test fracture specimens extracted from the pipe specimens (recall that the wall thickness for the utilized pipes is only 7.11 mm). Consequently, we proceed with the flaw assessment by adopting $K_{\mathrm{Ic}} = 155$ MPa$\sqrt{m}$ as the toughness value for the tested austenitic stainless steel.

5.2. BS 7910

The FAD methodology based upon the BS7910 Level 2 has also been applied to predict the burst pressure for the tested pipe specimens with the material toughness, K_{Ic}, taken as 155 MPa$\sqrt{m}$ [6]. While the FAD

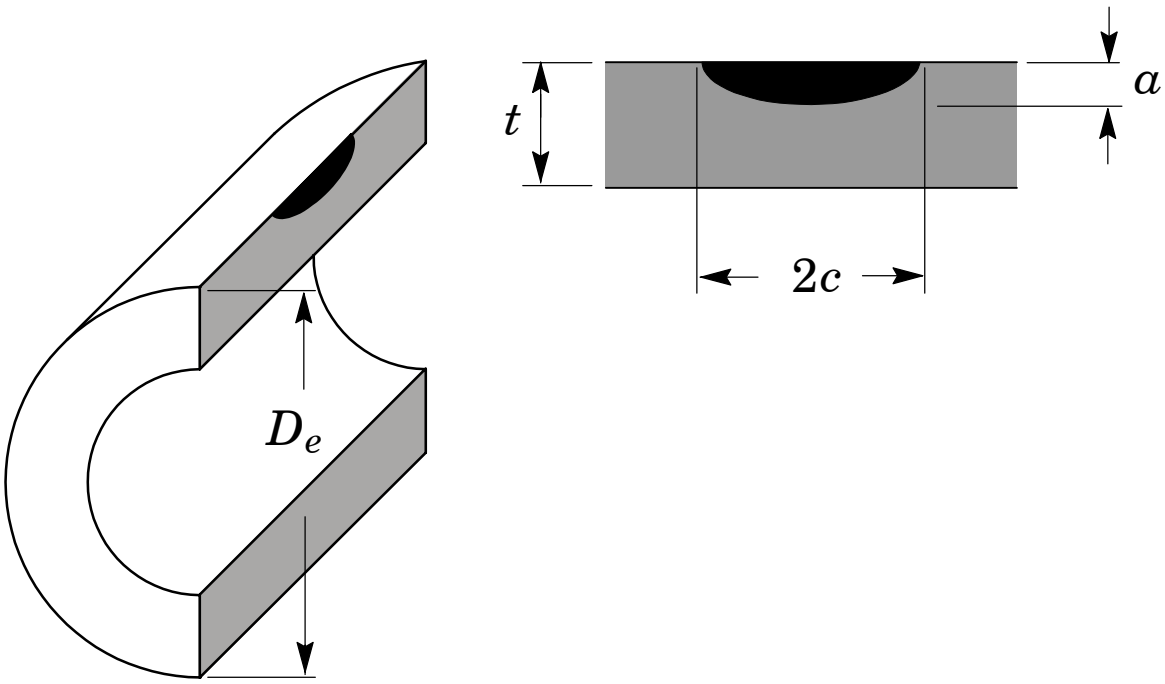

(a)

(b)

Figure 2 *(a) Pipe specimens with external axial flaws employed in the tests; (b) Test rig utilized for the hydrostatic testing..*

(a)

(b)

Figure 3 *Pipe failures after burst: (a) Specimen A2; (b) Specimen A3.*

equation is essentially similar to the corresponding curve for the API 579 procedure, there are some differences with respect to the calculation of the reference stress, σ_{ref}, and the stress intensity factor. Within the BS 7910 procedeure, the reference stress is given by

$$\sigma_{ref} = 1.2 M_S P_M \tag{13}$$

where P_M is the membrane stress acting on the crack face (opening mode) and parameter M_S is now expressed by

$$M_S = \frac{1 - \left[a/(tM_t)\right]}{1 - (a/t)} \tag{14}$$

with parameter M_t defined by

$$\left(1 + 1.6\frac{c^2}{R_i t}\right)^{0.5} \tag{15}$$

The stress intensity factors for the axially cracke pipes is calculated from the expression

$$K_{\mathrm{I}} = M f_W M_M P_M \sqrt{\pi a} \tag{16}$$

where coeficients M, f_W, and M_M are given by Anex D of BS 7910 for a cylindrical shell with a longitudinal, semi-elliptical flaw.

5.3. Burst Pressure Predictions

Figure 4 provides the predicted burst pressure for the tested pipes using the FAD methodology. The symbols in the plots represent the predicted values whereas the solid line defines equality between the experiments and predictions, *i.e.*, $P_{B-exp} = P_{B-pred}$. The plot includes both values for the predicted pressures; here, the open symbols represent the predicted values using API 579 whereas the full symbols represent the predicted values using BS 7910. Table 4 compares the predicted burst pressures for both procedures. While both procedures yield lower burst pressures compared to the experimentally measured values, the BS 7910 procedure provides unduly conservative values for the failure pressure.

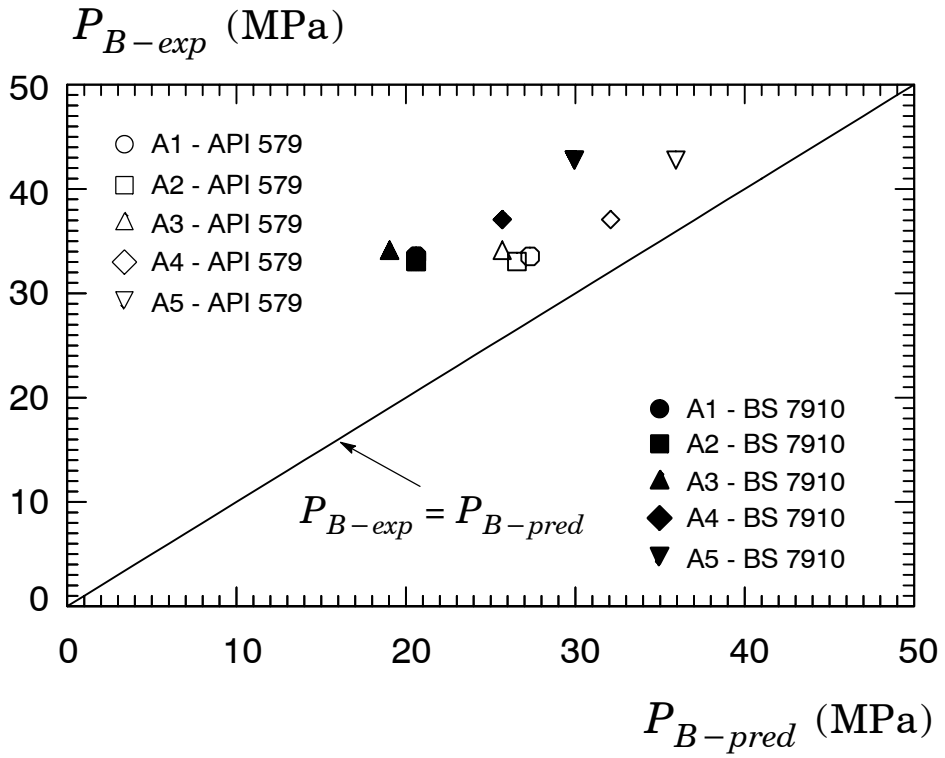

Figure 4 *Predicted burst pressures for the tested pipe specimens based upon API 579 and BS 7910.*

Table 4 Comparison between predicted burst pressure for tested pipes using API 579 and BS 7910

Specimen / Crack Geometry	A1	A2	A3	A4	A5
Measured Burst Pressure P_B (MPa)	33.5	33.0	34.1	37.1	42.8
Predicted Burst Pressure – API 579 P_B (MPa)	27.3	26.6	25.6	32.1	35.9
Predicted Burst Pressure – BS 7910 P_B (MPa)	20.6	20.6	19.0	25.7	29.9

6. Concluding Remarks

This study explores the applicability of failure analysis diagrams for failure assessments of austenitic steel pipes with axial flaws to include the effects of strain hardening properties and ductility. Full–scale burst tests are conducted on a 4 inch pipe made of AISI 304 steel containing different axial cracks to measure the failure pressure. The direct application of the API 579 and BS 7910 procedures indicate large margins between the predicted and the actual (measured) failure pressures. While such conservatism represents an extra factor of safety, excessive pessimism in defect assessments can lead to unwarranted repairs or replacement of in-service pipelines at great operational costs. These results provide support to develop more refined FAD procedures which are more applicable to austenitic stainless steels.

7. References

1. British Standard Institution. "Guide on Methods for Assessing the Acceptability of Flaws in Metallic Structures." BS7910, 1999.
2. American Petroleum Institute. "Recommended Practice for Fitness-for-Service." API RP-579, 2000.
3. Dowling, A. R. and Townley, C. H. A.., "The Effects of Defects on Structural Failure: A Two-Criteria Approach," *International Journal of Pressure Vessels and Piping*, Vol. 3, pp. 77-137, 1975.
4. Harrison, R. P., Loosemore, K. and Milne, I., "Assessment of the Integrity of Structures Containing Defects," *CEGB Report R-H-R6, Central Electricity Generating Board*, UK, 1976.
5. Milne, I., Ainsworth, R. A., Dowling, A. R. and Stewart, A. T., "Assessment of the Integrity of Structures Containing Defects," *CEGB Report R-H-R6-Revision 3, Central Electricity Generating Board*, UK, 1999.
6. *National Research Institute for Materials* (NRIM), Fracture Toughness Data for Austenitic Stainless Steels.

8. Responsibility Notice

The authors are the only responsible for the printed material included in this paper.